Proceedings of the 7th International Symposium on Cavitation
CAV2009
August 17-22, 2009, Ann Arbor, Michigan, USA

CAV2009 – Paper No. 35

Application of computer vision techniques to measure cavitation bubble volume and cavitating tip vortex diameter.

Luca Savio, Department of Naval Architecture and Marine Engineering (DINAV), Genoa University, Italy

Michele Viviani, Department of Naval Architecture and Marine Engineering (DINAV), Genoa University, Italy

Francesco Conti, Fincantieri C.N.I. Spa – Naval Vessel Business Unit - Genoa, Italy

Marco Ferrando, Department of Naval Architecture and Marine Engineering (DINAV), Genoa University, Italy

ABSTRACT

In present paper application of computer vision techniques to propeller cavitation experiments is presented. These techniques are widely adopted in many different environments and therefore they are well documented. They are also attractive from an economic point of view, due to relative low cost of the hardware involved.

Nevertheless their application to study propeller behavior in cavitation tunnel is not straightforward, because of the non-standard environment. However the adoption of these techniques may open a wide field of investigation and can result in a deepening of knowledge in propeller cavitation phenomena. In particular, obtained data can be linked to connected topics, such as propeller radiated noise or pressure signature, providing a better understanding on the sources of these effects, and invaluable information for validation of computer simulations.

Present paper traces a possible path to develop an experimental technique, covering theoretical points as well as data analysis strategies and other practical aspects. All techniques are presented through practical application, thus making clearer their points of strength and their shortcomings. Besides achieved results, possible improvements and future developments are outlined.

INTRODUCTION

Cavitation on propellers and hull appendages is one of the most important issues in hydrodynamic ship design. This importance is due to the increase in ship performance, not only considered in terms of speed, but also in terms of onboard comfort and environmental impact. Pressure pulses and radiated noise, which affect both characteristics, are well known effects of propeller cavitation.

Many different approaches to treat these phenomena are present in literature, but they are applicable once some quantities, that are difficult to be assessed, are known. These approaches, for instance, rely on variation of sheet cavitation volume or cavitating vortex diameter knowledge to predict pressure pulses and radiated noise level respectively.

More precisely, if sheet cavitation is concerned, in [1] a relation to predict pressure pulses due to bubble volume variation is reported

$$p_c \propto \frac{\rho}{4\pi R}\frac{\partial^2 V_b}{\partial t^2} \qquad (1)$$

Where p_c is pressure signature generated by the cavitation volume V_b variation at a given distance R.

In the tip vortex case the TVI (tip vortex index techniques) provides a mean to predict acoustic pressure p_a in a point at a distance R once the diameter D_v of the cavitating vortex is available

$$p_a \propto \frac{\rho}{R} Z^{0.5} \frac{\pi}{4} D_v^2 V_{tip} n \qquad (2)$$

Where Z is the blade number, V_{tip} can be assumed to be equal to the propeller radial velocity at tip, n is propeller's turning rate.

It has to be pointed out that these values could be evaluated nowadays by means of numerical codes, but besides the great achievement in this field there is still the need of experimental

results to validate calculated volumes (and in particular their variation during propeller turn) and diameters.

Computer vision techniques represent a promising set of tools, which are nowadays more and more applied in many different fields. In this paper techniques for passive volumetric reconstruction and active surface reconstruction are presented.

Volumetric reconstruction is obtained through "stereometry" or "shape from silhouette". In general, this technique is an image processing and 3D reconstruction based procedure to evaluate objects from two or more non collinear sights, taken by digital cameras. In this particular case, it is applied to cavitation bubble volume measurement. This technique was first applied to a 2D hydrofoil in [3]. It should be noted that since the time that work was produced, the world of image grabbing and processing evolved considerably, in terms of hardware and software libraries available, therefore nowadays this technique seems to be likely to produce interesting results also in the more complicated 3D propeller environment.

Surface reconstruction is performed through a standard stereo triangulation algorithm as described in [4-5-6].

These procedures are well known computer vision techniques, but their application to cavitation in a water channel is not straightforward, mainly due to the non standard optical path, complex propeller geometry and the limitation in camera position due to tunnel window configuration.

The aim of the present work is to present an application of these techniques to the propeller case tested in a water tunnel, clearly underlining their advantages, shortcomings and further work still needed to consolidate them. The procedure is described from its basis to more specific aspects, and some results are reported. The paper deals also with the principal experimental set-up problems and with the image processing procedures needed.

COMPUTER VISION BASIS

In present work, different computer vision techniques are described; for the sake of simplicity, they will be divided in three groups, in accordance to subsequent steps usually followed when they are applied:

1. Camera/stereo system calibration
2. Image segmentation
3. Reconstruction

Calibration is the step of assessing optical properties of every single camera and of the stereo system. This step is the same for both techniques and therefore following description holds for both of them.

Image segmentation is the procedure of extracting information from the acquired images, with the aim of finding object of interest inside the frames. Image segmentation is not strictly part of the vision algorithm, and applied technique and results are affected by illumination, cameras setup, subject of interest etc. Besides this clarification, however, problems that arise in image processing in a cavitation tunnel are common for most cases. As a consequence, an exposition of encountered problems and of solutions applied in our specific case, are deemed interesting in general. In particular an active and a passive technique are proposed in present paper.

The most important difference between active and passive strategy, is that in the active case the light source is meant to eliminate or reduce significantly the image processing step, whereas in the passive case the image processing part of the procedure becomes predominant on the other. In this work for the active surface reconstruction a triggered laser light source has been adopted, which results in a reduced effort for image segmentation, whereas the light source for volumetric reconstruction was a standard stroboscopic light, used also for visual observations.

Reconstruction differs significantly between stereometry and stereo triangulation, being the first one a 3D to 2D projection, whereas the second one a 2D to 3D back-projection, as explained in the following.

It must be noted that both techniques are based on the same camera mathematical model. The image processing and reconstruction procedures implemented in present paper make large use of the OpenCv computer vision library [5-6]. Next paragraph will deal with the camera model used by OpenCv, which is the standard pinhole model.

THE PINHOLE CAMERA MODEL

The pinhole model is a largely used camera model; although being simple it is able to represent correctly the behavior of standard cameras (for instance, catadioptric cameras are not included). This model is valid if light rays path is free and, as a consequence, world points are projected onto image through straight lines. Unfortunately this is not true in the cavitation tunnel environment, due to the presence of a double interface water-glass-air. This topic will be deepened later in the paper.
If this model holds, denoting world and the camera coordinate by **M** and **m** respectively the projection of a scene view is formed by projecting 3D points into the image plane using the perspective transformation (3):

$$m = C \bullet \begin{bmatrix} I & 0 \end{bmatrix} \bullet \begin{bmatrix} R & T \\ 0 & 1 \end{bmatrix} \bullet M \qquad (3)$$

Where C is the so called camera matrix which, for a camera working in a homogeneous mean, is an intrinsic property, I is the 3x3 identity matrix, R is the rotation matrix and T is the translation vector. Rotation and translation are relative to an arbitrary world frame of reference. More in detail the camera matrix has the form reported in (4)

$$C = \begin{bmatrix} f_x & 0 & c_x \\ 0 & f_y & c_y \\ 0 & 0 & 1 \end{bmatrix} \qquad (4)$$

Where f_x and f_y are the focal lengths along the x and the y axes respectively, c_x and c_y the optical centers. If these

properties are expressed in pixel units, the resulting vector **m** is the image indexes couple.

The model presented above is valid for an ideal camera, which is a camera fitted with lenses which do not produce optical distortions. Real lenses, on the contrary, always produce some optical distortion that can be divided in two categories: radial and tangential. The OpenCv provides tools to take into account effects of lenses.

The camera matrix and the optical distortion are called intrinsic parameters, because they do not change with respect to the camera pose, whereas rotation and translation are called extrinsic parameters. This holds, as mentioned before, until the pinhole camera model basic assumption of straight light rays is valid. In the cavitation tunnel environment the double interface water-glass-air causes the above assumption to be no more correct. In figures 1 and 2 the projection described in the pinhole model and the tunnel case are presented.

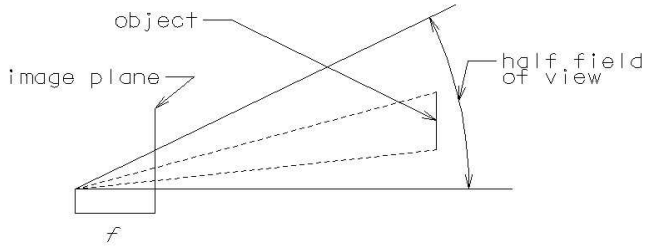

Figure 1 Projection in the pinhole camera model

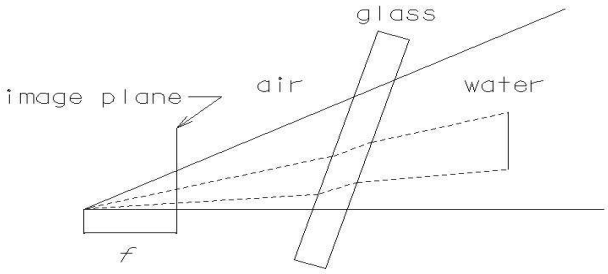

Figure 2 Cavitation tunnel optical path

As it can be seen from figure 2 the optical path from the 3D object to the image plane is not straight, but undergoes two refractions according to Snell's law. This issue can be overcome by considering the image provided by the camera as a photo of a virtual image, produced by the tunnel window, as shown in figure 3.

With this assumption, an image captured by the camera can be considered as a "photo of a photo", in which the transformation between the first and the second photo is a homography or projective transformation.

A homography, in the pinhole framework, represents the transformation between two images of the same planar object.

If we denote the 3x3 homography matrix with **H** the image coordinate **m** obtained through (3) will be remapped in coordinate **m'** by relation (5):

$$m' = H \bullet m \qquad (5)$$

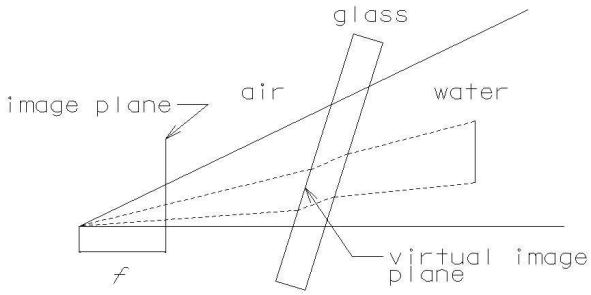

Figure 3 Virtual image plane

Therefore the homography for a particular camera setup can be computed by images of the same planar object (for this purpose the calibration pattern was employed) inside the cavitation tunnel, at first when water is not present and then when the tunnel is filled. Figure 4 shows the calibration pattern in the tunnel without water (left), with water (right) and than the results of applying the homography to the one with water in order to eliminate double interface effect, showing the considerably good result. It can be pointed out that this transformation holds for a particular calibration pattern position, or only for a limited space around this position: The same holds also for extrinsic parameters of the stereo system, as it will be clarified later, and therefore no particular restriction to the setup is added.

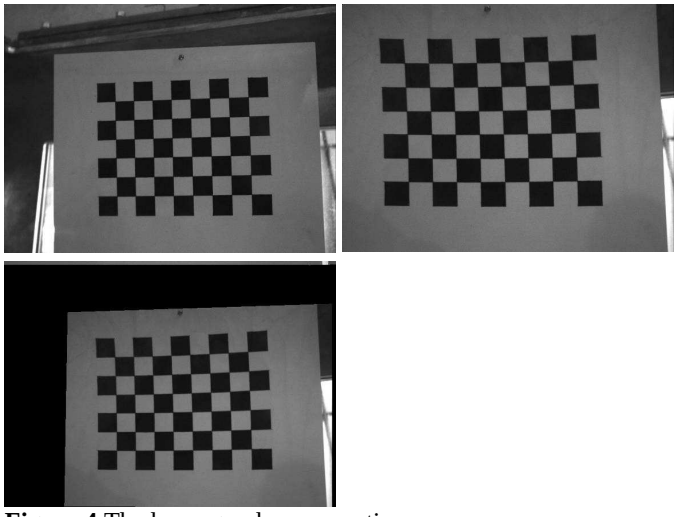

Figure 4 The homography assumption

It can be noticed that in this procedure distortions caused by tunnel window are neglected, but at this preliminary stage the important point is that now the pinhole model holds for virtual images pairs.

CAMERA CALIBRATION

Camera calibration is the procedure used to obtain optical properties of a single camera, which means finding intrinsic and extrinsic parameters. Second ones are rotation and

translation referred to an arbitrary world coordinate frame of reference. This aspect will not be covered in detail because OpenCv offers full support to perform both intrinsic and extrinsic calibration. Only the steps to be accomplished will be exposed.

As a first step, optical properties of each single camera must be assessed, i.e. camera matrix and optical distortion coefficients have to be computed. This task is carried out by mean of a set of images of an object whose geometry is known (named calibration pattern or calibration rig). The images should cover the full camera field of view (FOV), in order to obtain reliable results. Although the calibration pattern could be arbitrary the OpenCv provides built-in support for planar chessboard as shown in figure (5).

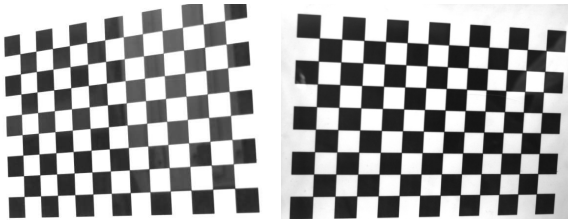

Figure 5 Calibration pattern

Once intrinsic parameters are known, extrinsic ones can be calculated. As mentioned before camera rotation and translation could be referred to an arbitrary world frame of reference. If a stereo system is concerned, as in present case, among possible choices the most common is to refer coordinate of the second camera to the first one. With this choice extrinsic parameters of reference camera are fixed, being rotation the identity matrix and translation the null vector. Calibration is carried out by taking a large set of images in which the pattern is visible by both cameras, with different poses. It must be noticed that, even if from a theoretical point of view extrinsic parameters are determined for every scene that the stereo system could capture, in reality only a finite volume is calibrated correctly. This is due to the fact that an optimization algorithm is embedded in every calibration algorithm, and therefore best results will be obtained only in the region of space (attached to camera reference frame) in which the pattern was captured. This explains the fact that adding the homography to the projection procedures does not limit substantially the technique, being both limited to a region in space.

These general considerations are valid for both techniques, but some specific aspects must be analyzed. One of the most important features is the distance between cameras optical centers, generally addressed as base line. A large base line is important to obtain good reconstructions, but could cause problems in the case of stereo triangulation, because matching corresponding points in the two images could become difficult if the two scenes differ significantly. On the other hand, when stereometry is adopted, the two scenes must provide as many as possible different information, thus they should differ significantly one from the other. As a result, a good camera setup for stereometry is not generally good for stereo triangulation and vice versa. This leads to the adoption of different cameras setup according to the technique in use, as reported schematically in Appendix A.

STEREOMETRY: TECNIQUE OUTLINE

"Stereometry", also named "shape from silhouette", is a technique that enables a volumetric reconstruction by the knowledge of two or more different sights of an object. In other words it is a reconstruction based on the projections of the object on multiple planes, similar to technical drawing, which is a particular case where projections are orthogonal as well as planes relative position and orientation. In figure 6 a 2D representation of the technique is given.

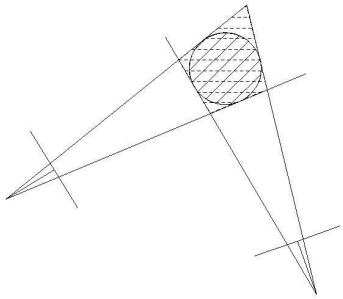

Figure 6 "Stereometry" 2D representation

By observing figure 6 it can be pointed out that the reconstruction error can be high for flat object (quasi 2D object). Nevertheless, it must also be noticed that this technique does not suffer from the occlusion issue and therefore it is able to provide some information also in regions that are not directly accessible by cameras. The reconstruction error, which can be high, could be theoretically reduced by increasing the number of views. This, however, presents some practical problems, because an increase in camera number requires a higher precision in calibration parameters, which is currently very difficult to achieve. This explains the reason why, notwithstanding the fact that several attempts were carried out during present research, in this paper only results obtained adopting two cameras were used. Cameras number increase is still a research topic under study.

STEREOMETRY: SEGMENTATION

This step corresponds to locating in the images the object to be reconstructed, in our case the cavitation bubble.

Many general techniques are available for segmentation, but there is still the need to customize them to this particular application, since these algorithms are commonly applied in completely different situations. If we consider figure (7 left) sheet and tip vortex cavitation are clearly visible, but the incoming flow carries a number of passing bubbles which are not linked to propeller cavitation. These travelling bubbles must be eliminated, since otherwise the image gradient would result in a noisy map (7 right), where it is almost impossible to trace propeller cavitation. A common set of image processing algorithms have the aim of finding objects which move in static scene (consider for example a video surveillance or traffic surveillance camera). This explains the need of creating customized tools for the cavitation tunnel environment.

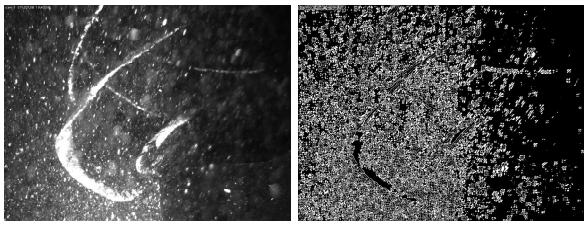

Figure 7 Typical effect of taking the image gradient

An important point is the illumination. Illumination determines the strategy in carrying out segmentation. In present work a common gas flash lamp was used, triggered with propeller turning, illuminating the bubble from a direction that was approximately perpendicular to camera sights. This configuration was chosen because it provided satisfactory results. It is believed that improvements can be obtained if more light sources are adopted; this matter will be object of future investigations.

Once satisfactory images have been taken, first of all it is necessary to eliminate propeller blades, shaft etc. This can be done by subtracting a background image of the non cavitating propeller to each single image.

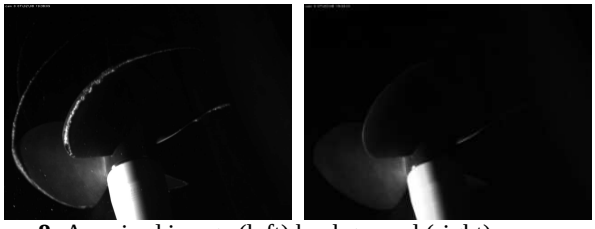

Figure 8: Acquired image (left) background (right)

Resulting images are generally noisy, therefore a median filter is applied.

As already pointed out, in water tunnel there are also bubbles in the incoming flow, which are not easy to distinguish from the propeller bubbles, because they share identical optical properties. These bubbles can be eliminated by analyzing the mean of several images instead of a single one, considering the fact that bubbles move while cavitation bubble is stationary. The resulting image is named as “mean bubble”. This is also consistent with the research aim of analyzing global and time averaged effects. Typically, depending on the amount of passing bubbles, the mean is performed over 5 to 10 images.

Figure 9: Mean bubble

At this stage a good image is obtained but it has to be noted that the image is still a grey level image. The next step is to precisely define the region of the image where the bubble extends. A simple threshold of the image would lead to a noisy image, if the threshold is too low, or to leave out bubble’s boundaries, if the threshold is too high. A solution is to combine by means of fuzzy logic these two facts:

- On the boundaries the image gradient is high.
- In the bubble interior the gray level is higher than the mean image grey level.

The fuzzy logic core is the membership function that, for both criteria, was chosen to be the sigmoid right as reported in equation (6) and shown in figure (10)

$$\mu(u,v) = \frac{1}{1+e^{-(gl-M-\sigma)/\sigma}} \qquad (6)$$
$$0 \le \mu(u,v) \le 1$$

Where *(u,v)* are pixel coordinate, *gl* is the pixel grey level, *M* is the image mean grey level and σ the image standard deviation. As it can be seen from figure (10) this membership function acts as a threshold for low level of image standard deviation, whereas is more conservative for noisy image where the standard deviation is higher. A value of 0.5 is assigned to a pixel having a grey level equal to the mean image grey level plus the image grey level standard deviation.

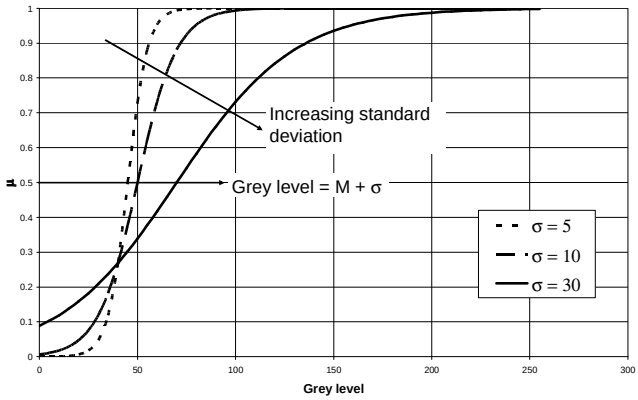

Figure 10 Sigmoid right membership function

Once the fuzzy set is created, it must be de-fuzzy. The technique employed here consists in applying a fixed threshold to weighted sum of two criteria. This results in a binary image, which is an image where bubble pixels are white, whereas other pixels are black.

Figure 11: Segmented image

STEREOMETRY: RECONSTRUCTION

Reconstruction is carried out in two subsequent steps. A rectangular 3D point grid is created in the world frame of reference. These points are projected onto the image plane; if a

point is projected onto a white pixel it is kept, otherwise it is cancelled. Repeating this procedure for every camera, only grid points belonging to the bubble survive the projection process. With this first step, an initial estimation of the 3D bubble shape and of its volume is obtained. The grid for memory reason at this stage is coarse as it can be seen from figure 12, being typically formed by 10^6 voxels (i.e. volume elements).

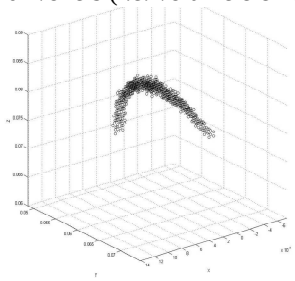

Figure 12: Coarse grid

This first grid has the only aim to define the region of space belonging to the bubble. As a second step, a refined grid is created using the coarse one as basis. This grid has a spatial step chosen according to coarse bubble volume. Refined grid is defined following subsequent steps:

- Coarse bubble is cut into sections
- Each section is analyzed finding area center and convex hull
- Each section is re-meshed according to previously defined spatial step

Once the fine grid has been defined, this is reanalyzed following the procedure described for the coarse one. Result of the procedure is shown in figure (13).

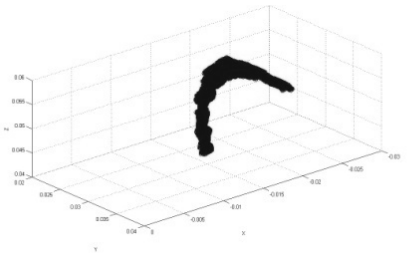

Figure 13: Reconstruction (refined grid)

FIRST APPLICATION

The outlined technique was applied to a stock propeller tested in the cavitation tunnel of the University of Genoa (see Appendix A).

In figure 14 sheet cavitation volumes against cavitation index at a fixed advance coefficient are presented.

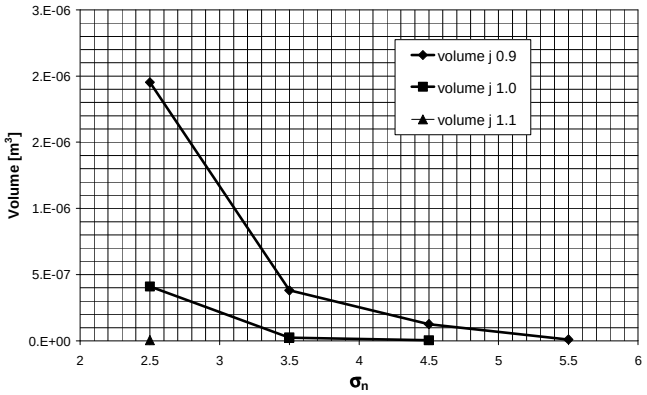

Figure 14 Sheet cavitation volume at different advance coefficients and cavitation index

Volume variation seems to be captured although, as mentioned before, this technique is not suitable for quasi-2D objects. Reconstruction error could be high and difficult to be assessed, but being manly linked to cameras setup, it could be considered constant for objects with similar shape. Hence stereometry may be used in this case not for actual volume measurement, but for comparison of volumes connected to different propeller geometries.

In order to overcome this problem, considering that sheet cavitation by its nature adheres to propeller blade, it was deemed possible to obtain a volume estimation considering the volume between bubble surface and blade surface. This led to the development of the stereo triangulation approach, which will be covered in the last part of paper.

When cavitating tip vortex is concerned it is possible to employ stereometry as a useful research tool. First of all, tip vortex is a 3D object, being mostly cylindrical, thus being more suitable than a predominantly 2D object for stereometry application. Secondly it develops in the propeller down stream, so it does not adhere to any object, resulting in difficulties for application of other techniques. In this case, moreover, some operational advantages make this technique attractive:

- The background is in general limited (only tunnel's walls if visible).
- The sights are free from blade occlusion, and therefore cameras can be set more freely.

Besides these advantages, however, some problems exist:

- Tip vortex is less stable than sheet cavitation, especially at inception, fluctuating in space. As a consequence, the mean of a large set of images could cover a region of space more extended than the real one, resulting in a diameter over-estimation
- More than one coil could be visible in a single image, leading to reconstruction ambiguity.

The first point leads to reduce the number of images used in defining the so called mean bubble; as a consequence travelling bubbles could remain after image segmentation.

The second point can be avoided if a Region of Interest (ROI) is applied to each image. In figure (15) the original acquired images are reported, showing that the background is almost totally absent and that sights are not obstructed by propeller blade, shaft, etc. On the other hand, more than one coil is visible, apparently intersecting, limiting the region where reconstruction is possible. Figure (16) reports the result of segmentation without setting a ROI, while in figure (17) a ROI is chosen.

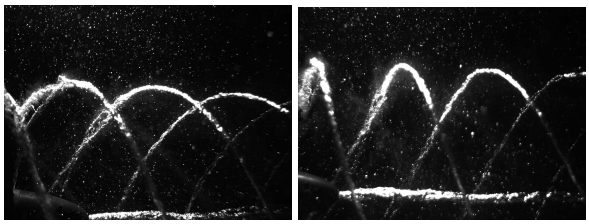

Figure 15 Cavitating tip vortex at low cavitation index

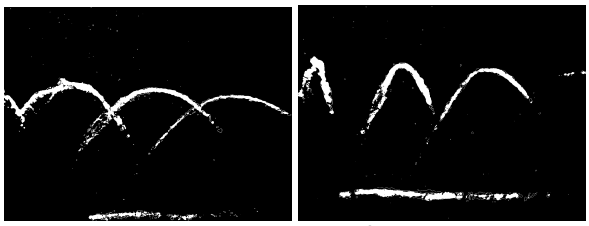

Figure 16 Segmented images left and right camera

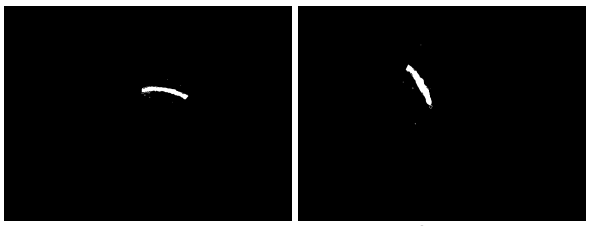

Figure 17 Segmented images with ROI left and right camera

The reconstructed vortex is presented in figure (18): as it can be seen, the shape is reasonably well captured.

As stated in the introduction main interest is determination of vortex diameter, but at this stage only a volumetric reconstruction is available, hence some post processing is required. In present work, a preliminary attempt to measure diameter from the reconstructed bubbles is presented. The basic idea is that the area of a bubble section is proportional to the square root of the vortex diameter which generated it. Therefore bubble is cut into sections and each section is analyzed evaluating sectional area and area center. It has to be remarked that area center is necessary in this process because the vortex axis is needed for a correct analysis. In particular, being grid sections referred to the cameras reference frame, sectional area must be projected on a plane that locally is perpendicular to vortex axis.

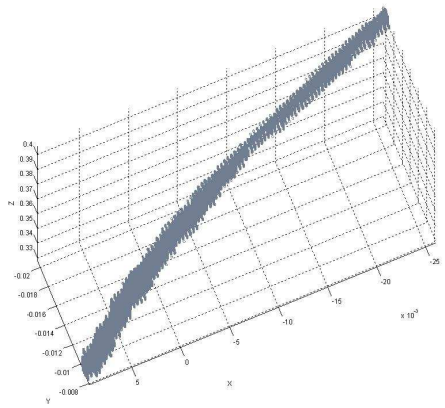

Figure 18 Reconstructed vortex

Results are reported in figure 19, where the vortex diameter dependence on propeller load (through the advance coefficient J) and on cavitation index σ_n is clearly visible. This is in accordance to what is physically expected, despite preliminary nature of the procedure applied to obtain vortex diameter from reconstructed volume. Future work will include a validation with objects of known diameter in order to quantify measurement errors.

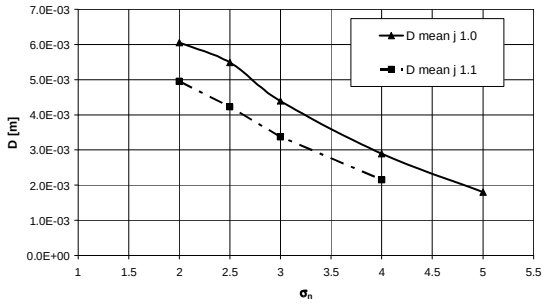

Figure 19 Vortex diameter against cavitation index

Standard deviation of diameter provides an estimate of vortex instability. Figure (20) shows that high cavitation numbers, near inception, are connected to larger local variation of diameter, while scatter decreases with the increasing vortex stability. This is also confirmed by the dependence on propeller load.

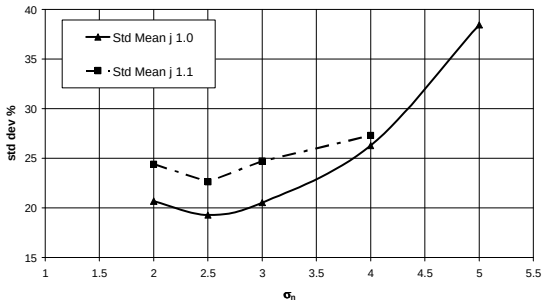

Figure 20 Vortex diameter standard deviation

ACTIVE STEREO TRIANGULATION: INTRODUCTION

Stereometry, despite performing a volumetric reconstruction directly, has the shortcoming that experimental error can be high and moreover difficult to assess. As stated before error could become unacceptable for quasi 2D objects. A solution to this problem is to adopt a technique which enables a surface reconstruction. Obviously, if a volume is needed, two limiting surfaces are necessary. If sheet cavitation is concerned, these two surfaces are represented by bubble and blade surfaces.

In present work, therefore, a study on the feasibility of a surface reconstruction technique is presented.

Stereo triangulation is a widely adopted technique to reconstruct 3D surfaces and it is theoretically simple, but suffers from the difficulty of the so called stereo matching, which is the procedure of finding corresponding points in stereo images. In order to perform stereo matching, images texture or some conspicuous points are required. Unfortunately, sheet cavitation does not provide, in general, any of them. To overcome this problem a conspicuous point can be artificially created, and hence the technique is active, by projecting a light ray or a texture with a coded light pattern. Although the second is preferable, since it can reduce experimental time, in the cavitation tunnel environment it is difficult to be realized, due to light absorption caused by water. A concentrated light is the easiest and cheapest solution, therefore a laser source, triggered with propeller rotation, was adopted.

The proposed procedure, which is currently at a preliminary stage and still lacks an extensive validation campaign, can be described as follows:

- At a given blade angle a blade surface reconstruction is performed, in non cavitating conditions.
- At the same blade angle a bubble surface reconstruction is performed at a particular cavitation index
- Bubble volume and thickness are computed by considering the space wrapped by the two surfaces.

In present work only a first application is presented, showing that this technique is promising.

It must be noted that reconstruction errors in this technique are easy to be determined and that they are mainly linked to base line length and calibration quality. In a preliminary phase a campaign, meant to determine reconstruction errors, was carried out, showing that, taking the calibration pattern as reference, its geometry is reconstructed with an error that is always less than 6% and in most cases lower than 2%. This error is defined as the ratio between reconstructed distance of two adjacent corners and the actual one. In figure (21) the error defined before is reported as a map over the calibration pattern. Since the procedure does not depend in this case on object shape, it is reasonable to consider a comparable accuracy also for blade and bubble reconstruction.

It must also be noted that this error is relative to the shorter baseline used in present study. Reconstructions presented later in the paper were obtained with a larger baseline, whose effect is to reduce reconstruction error.

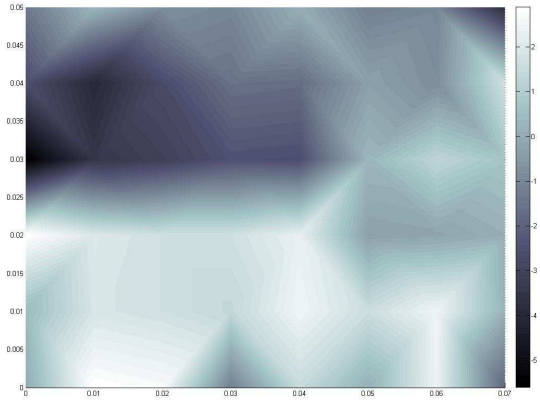

Figure 21 Reconstruction error

ACTIVE STEREO TRIANGULATION: GEOMETRY

Stereo triangulation is an application of triangulation in the framework of computer vision. If the pinhole camera model holds, stereo triangulation consists in finding intersection between light rays which are recognized as projections of the same 3D point on the two image planes. The perspective projection, in the most general case considered by the pinhole model, can be expressed by the so called Perspective Projection Matrix (PPM). Considering the projection transformation in (3) the PPM has the expression reported in (7):

$$PPM = C \bullet \begin{bmatrix} I & 0 \end{bmatrix} \bullet \begin{bmatrix} R & T \\ 0 & 1 \end{bmatrix} \tag{7}$$

For a given pixel, projection of a 3D point M, defined by coordinate (u,v) in the image plane, the equation of a ray passing through camera center is:

$$\begin{cases} (p_1 - up_3)^T M = 0 \\ (p_2 - vp_3)^T M = 0 \end{cases} \tag{8}$$

Where p_n denotes the n^{th} row of PPM and T the transposed matrix. This set of equation could be written also for the second camera denoted in (9) by an apex. Combining these two sets of equations a linear system of 4 equations in 4 unknowns is obtained.

$$\begin{cases} (p_1 - up_3)^T M = 0 \\ (p_2 - vp_3)^T M = 0 \\ (p'_1 - u' p'_3)^T M = 0 \\ (p'_2 - v' p'_3)^T M = 0 \end{cases} \tag{9}$$

The solution of this system provides world coordinates of the 3D point, whose projection are pixel (u,v) and (u',v') in the first and in the second image plane respectively. It has to be noticed that the adoption of these equations implies that the two pairs of coordinates are recognized in some way as projections of the same world point. Next paragraph will cover this problem.

ACTIVE STEREO TRIANGULATION: STEREO MATCHING

Stereo matching is the operation of finding corresponding points in a stereo pair, projection of the same 3D point. This operation is simplified if an active light source is adopted. In present work a laser source, triggered with propeller turning rate was used. The light source creates a light dot on the surface to be analyzed. No illumination is present in order to obtain a dark frame with only the dot visible. Nevertheless some problems were encountered, as explained in the following.

First of all, the laser beam, in correspondence to some positions, was reflected by tunnel windows, with the result that more than one dot was visible in one image. This ambiguity can be avoided applying a property of stereo cameras, addressed as epipolar constraint.

The epipolar constraint states that in a stereo pair, if a point **m** is recognized as projection of a world point **M,** its corresponding point in the other image lays on a line, named epipolar line. In figure 22 the epipolar line **e** is the intersection between the plane Π which contains the base line **b** and the stereo candidate **m** in the first image, and the second image plane.

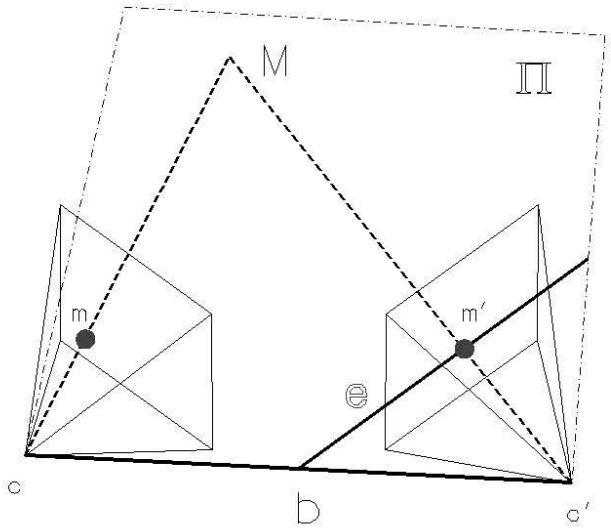

Figure 22 Epipolar geometry

In figure 23 a stereo pair is presented, showing the epipolar line for left image, corresponding to white dot in right one.

At this preliminary stage finding the dot inside the image is an operation carried out by the operator (thus being time consuming and possibly affected by errors), but in future machine learning algorithm are likely to replace this step improving process quality. The epipolar constraint is crucial in finding matching points, because it reduces the problem to a 1D problem, instead of a 2D problem.

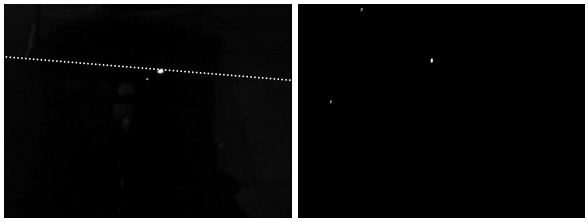

Figure 23 Epipolar constraint application

Once the dot is found inside the image, its area center is calculated and than used, together with the one deriving from the other image, to reconstruct the 3D point.

ACTIVE STEREO TRIANGULATION: RECONSTRUCTION

In order to obtain a good reconstruction of propeller blade, at least 100 points are needed, whereas the number of point for bubble reconstruction depends on its extension. These corresponding points are found in the virtual image plane. Once the homography is applied the reconstruction can be carried out.

System (9) does not have in general a solution since, due to calibration errors, the two rays do not intersect each other. Solution is found, in a least squares sense, by singular value decomposition of coefficient matrix.

In figure (24) the reconstructed blade back side is shown. It must be noted that blade was reconstructed only from a radius of about 0.5 R to the tip, because cavitation was expected in that region.

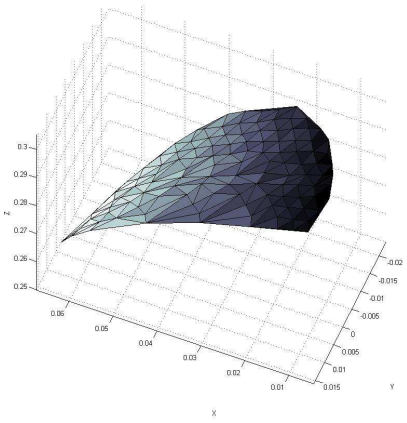

Figure 24 Propeller blade reconstruction

In figure (25) the two sets of points (for left and right camera) used for generating surface blade in figure (24) are plotted, showing refinement near propeller leading edge (left in both images) and towards propeller tip.

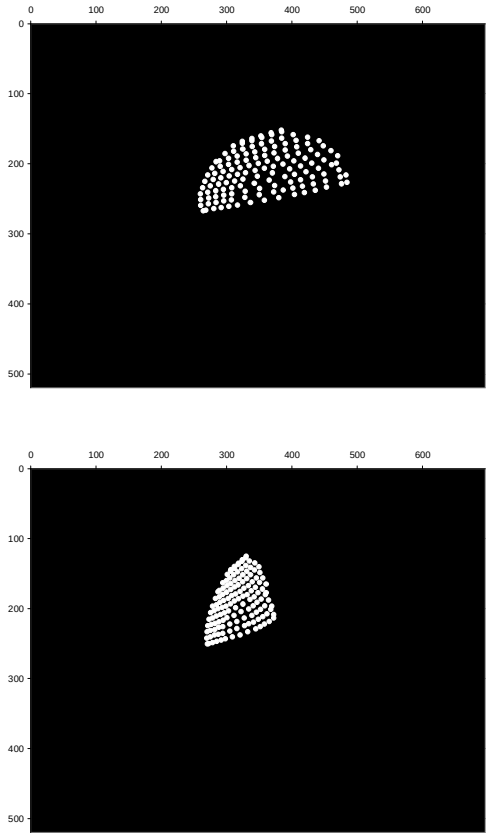

Figure 25 Left camera points set (up) – right camera set (below)

The same technique was applied to sheet cavitation bubble. Once the two surfaces are available bubble thickness can be computed. First step is to perform a Delaunay tessellation of the blade, in order to define planes which approximate local geometry. The second step consists of finding the nearest plane to each bubble point. Finally, local thickness is found as point distance from the nearest plane. In figure (26), computed thicknesses are reported, showing, for instance, that thickness increases in the tip region (bottom left).

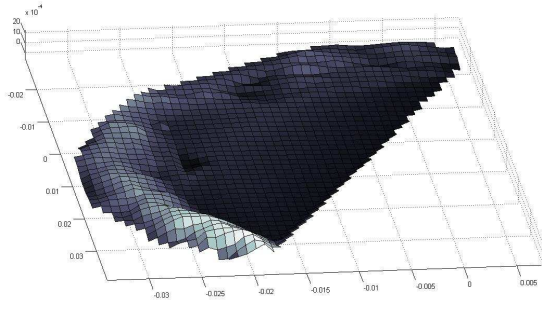

Figure 26 Sheet cavitation thicknesses

ACTIVE STEREO TRIANGULATION: CONCLUSIONS

Active stereo triangulation technique presented here is still at a preliminary stage; nevertheless some consideration can be already made.

Being an active technique, the effort in image segmentation is limited, thus resulting in a shorter development time. Currently, segmentation is performed mostly by the human operator. A possible improvement of the technique can be the development of a machine learning algorithm suitable for this application.

Reconstruction error, for a quasi-2D object, is limited and easily controllable, being linked to calibration parameters.

The biggest issue is that cavitation bubble, in some points, seams to be transparent to laser beam, or particularly sensitive to beam incidence angle. Due to lack of time, an extensive study on this subject cannot be presented here, but this problem has certainly to be considered with particular care in future.

Another issue is that if a single laser beam is adopted, the experimental time is rather high. For this reason another research topic is the creation of coded light pattern on the propeller and on the bubble.

Stereo triangulation could also be merged with strereometry. If sheet cavitation is considered, the reconstruction error arising from strereometry could be reduced if the propeller blade surface is set as limiting surface, as presented schematically in figure (27). In this case the resulting technique could be less precise than stereo triangulation, but faster from the experimental point of view.

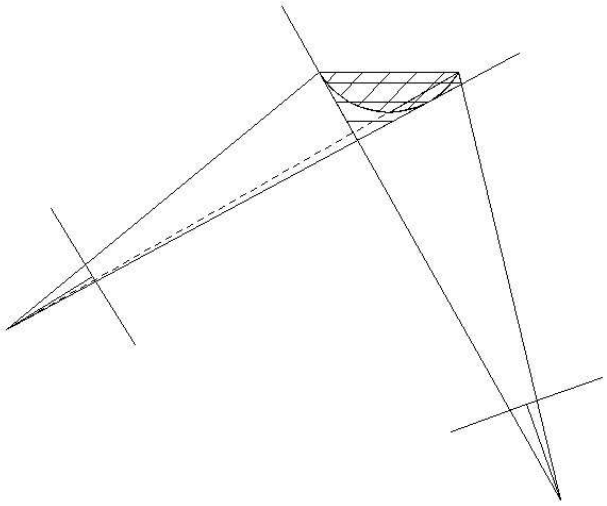

Figure 27 Stereometry with limiting surface

CONCLUSIONS

In the present work, two different vision algorithms are presented, analyzing them both from theoretical point of view and in their practical application. Specific aspects related to their use in a cavitation tunnel are covered, showing their merits and shortcomings.

Results are considered promising, since it was possible to obtain reasonable results in terms both of tip vortex diameter and of sheet cavitation volume reconstruction. In particular, active stereo triangulation seems to be the most promising technique for sheet cavitation measurement, while stereometry seems more suitable for tip vortex diameter.

Both procedures still present some shortcomings as discussed in the paper, and in future they will be further investigated.

Moreover, both methods rely on the pinhole camera model, which is one among a set of possible choices. More refined models are available, for instance some catadioptric model could be useful in representing correctly the actual ray path inside the cavitation tunnel.

Once the techniques will be consolidated, they will be applied to different propeller geometries with the aim of deepening the knowledge about relations between propeller cavitation patterns and resulting radiated pressure pulses and noise.

REFERENCES

[1] Carlton, J.S. *"Marine Propellers and propulsion"*, Butterworth-Heinemann, 2nd edition September 2007.

[2] Ræstad, A.E. *"Tip Vortex Index – an engineering approach to propeller noise prediction"*, 1996 The Naval Architect, Royal institution of Naval Architects.

[3] Pereira, F. *"Prèdiction de l'èrosion de cavitation: approche ènergètique" Ph.D thesis EPFL*, 1997.

[4] Hartley, R. and Zisserman, A. *"Multiple View Geometry in Computer Vision*" Cambridge University Press, 2nd edition, 2003.

[5] OpenCv Reference Manual

[6] Rost Bradski, G. and Kaehler, A., *"Learning OpenCv. Computer Vision with the OpenCV Library"*, September 2008, O'Reilly

[7] Fusiello, A. *"Elements of Geometric Computer Vision"* April 2008, http://www.sci.univr.it/~fusiello

[8] Caponnetto M., Brizzolara S. (1995a) '*Theory and Experimental Validation of a Surface Panel Method for the Analysis of Cavitating Propellers in Steady Flow*' Proceedings Propcav '95, 16-18 May 1995, Newcastle Upon Tyne.

[9] Caponnetto M., Ferrando M., Fioravanti G., Grossi L., Matera F., Podenzana-Bonvino C. (1995b) '*Propeller blade sections with enlarged cavitation bucket*' Proceedings Propcav '95, 16-18 May 1995, Newcastle Upon Tyne.

APPENDIX A

Experiments have been carried out at the Cavitation Tunnel facility of the Department of Naval Architecture and Marine Engineering of the University of Genoa (DINAV), represented in figure 28. The facility is a Kempf & Remmers closed water circuit tunnel with a squared testing section of 0.57 m x 0.57 m, having a total length of 2 m. Optical access to the testing section is possible through large windows.

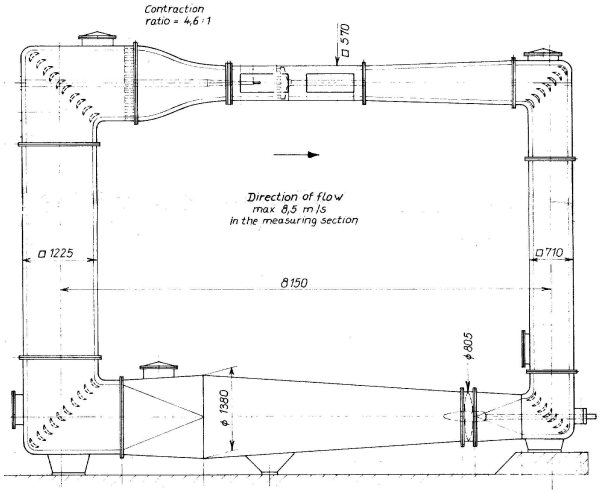

Figure 28: DINAV Cavitation Tunnel

The nozzle contraction ratio is 4.6:1, and the maximum flow speed in the testing section is 8.5 m/s. Vertical distance between horizontal ducts is 4.54 m, while horizontal distance between vertical ducts is 8.15 m. Flow speed in the testing section is measured by means of a differential Venturimeter with two pressure plugs immediately upstream and downstream of the converging part, or by Pitot tube (the latter normally adopted when surface piercing propellers are tested). A depressurization system allows obtaining an atmospheric pressure in the circuit near to vacuum, in order to simulate the correct cavitation index for the tests.

Video cameras used for stereo vision are two standard Allied Vision Technology Marlin 145B2. Cameras setup adopted in present work for stereometry and stereo triangulation are schematically reported in figure 29 and 30 respectively. From these figures, the large base line adopted for stereometry, in order to reduce reconstruction error, and the shorter base line for stereo triangulation, whose aim is to facilitate stereo matching, can be noticed. The stroboscopic lamp is positioned slightly upstream the propeller under the lower tunnel window. On the contrary the laser source was positioned approximately between the two cameras, mounted on a three axes computer controlled traverse system, whose aim is to provide high resolution movements.

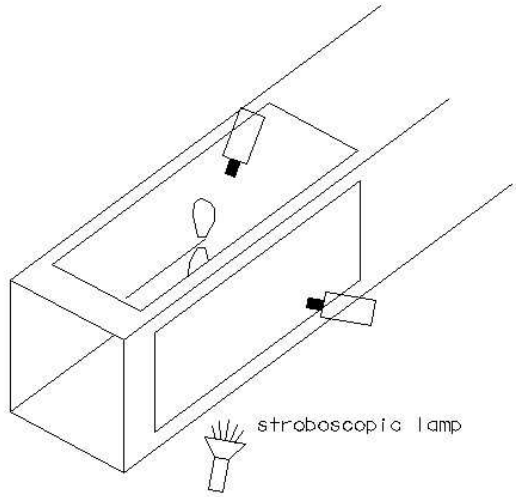

Figure 29 Cameras setup for stereometry

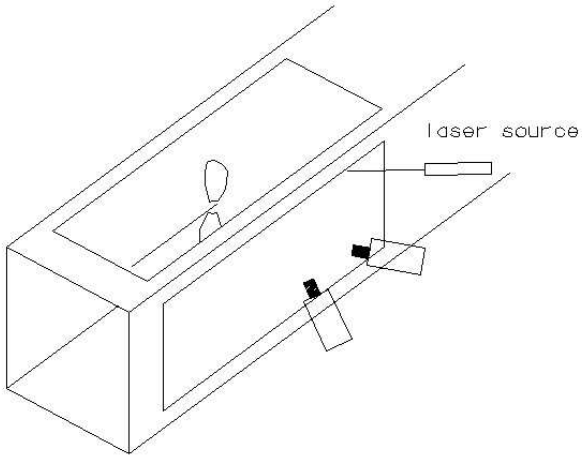

Figure 30 Cameras setup for stereo triangulation

r/R	c/D	sk [°]	rake	P/D	t/c	f/c
0.2	0.2192	0.0000	-0.0131	1.3299	0.1979	0.0000
0.25	0.2479	-1.0000	-0.0204	1.3591	0.1649	0.0076
0.3	0.2714	-1.6860	-0.0262	1.3883	0.1361	0.0121
0.4	0.3184	-1.6430	-0.0329	1.4426	0.0907	0.0179
0.5	0.3706	-1.4510	-0.0393	1.4927	0.0598	0.0206
0.6	0.4222	-1.2990	-0.0463	1.5177	0.0381	0.0213
0.7	0.4353	0.0000	-0.0482	1.5094	0.0258	0.0213
0.8	0.4091	2.7520	-0.0413	1.4743	0.0165	0.0212
0.85	0.3653	4.9210	-0.0351	1.4426	0.0144	0.0218
0.9	0.3027	7.2280	-0.0290	1.3967	0.0124	0.0230
0.95	0.2009	9.8530	-0.0204	1.3382	0.0124	0.0235
1	0.0500	13.2040	-0.0111	1.2505	0.0124	0.0000

Table 1 E033 parameters

The propeller used for experiments is the E033 propeller designed by Cetena, whose main geometrical parameters are reported in table (1).

The propeller has a diameter of 0.227 m and it was tested at a constant turning rate of 22.5 Hz. Shaft inclination was set to 4° Open water characteristics, relative to operating conditions presented in the paper, are reported in figure 31 and table (2)

J	Kt	$10xK_Q$	η_0
0.90	0.323	0.735	0.630
0.95	0.297	0.684	0.656
1.00	0.274	0.641	0.680
1.05	0.247	0.593	0.699
1.11	0.224	0.551	0.718

Table 2 Open water characteristics

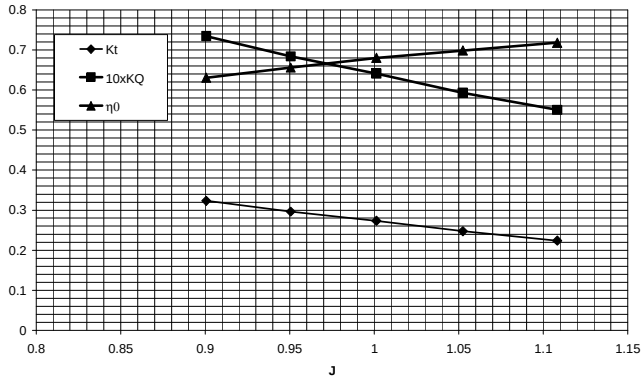

Figure 31 Open water characteristics